SCIENCE CHINA
Earth Sciences

• RESEARCH PAPER •

January 2014 Vol.57 No.1: 1–12
doi: 10.1007/s11430-014-4994-1

# Using CMIP5 model outputs to investigate the initial errors that cause the "spring predictability barrier" for El Niño events

ZHANG Jing[1], DUAN WanSuo[2*] & ZHI XieFei[1]

[1] *Key Laboratory of Meteorological Disaster of Ministry of Education, Nanjing University of Information Science & Technology, Nanjing 210044, China;*
[2] *State Key Laboratory of Numerical Modeling for Atmospheric Sciences and Geophysical Fluid Dynamics (LASG), Institute of Atmospheric Physics, Chinese Academy of Sciences, Beijing 100029, China*

Received August 19, 2014; accepted October 8, 2014

Most ocean-atmosphere coupled models have difficulty in predicting the El Niño-Southern Oscillation (ENSO) when starting from the boreal spring season. However, the cause of this spring predictability barrier (SPB) phenomenon remains elusive. We investigated the spatial characteristics of optimal initial errors that cause a significant SPB for El Niño events by using the monthly mean data of the pre-industrial (PI) control runs from several models in CMIP5 experiments. The results indicated that the SPB-related optimal initial errors often present an SST pattern with positive errors in the central-eastern equatorial Pacific, and a subsurface temperature pattern with positive errors in the upper layers of the eastern equatorial Pacific, and negative errors in the lower layers of the western equatorial Pacific. The SPB-related optimal initial errors exhibit a typical La Niña-like evolving mode, ultimately causing a large but negative prediction error of the Niño-3.4 SST anomalies for El Niño events. The negative prediction errors were found to originate from the lower layers of the western equatorial Pacific and then grow to be large in the eastern equatorial Pacific. It is therefore reasonable to suggest that the El Niño predictions may be most sensitive to the initial errors of temperature in the subsurface layers of the western equatorial Pacific and the Niño-3.4 region, thus possibly representing sensitive areas for adaptive observation. That is, if additional observations were to be preferentially deployed in these two regions, it might be possible to avoid large prediction errors for El Niño and generate a better forecast than one based on additional observations targeted elsewhere. Moreover, we also confirmed that the SPB-related optimal initial errors bear a strong resemblance to the optimal precursory disturbance for El Niño and La Niña events. This indicated that improvement of the observation network by additional observations in the identified sensitive areas would also be helpful in detecting the signals provided by the precursory disturbance, which may greatly improve the ENSO prediction skill.

**El Niño-Southern Oscillation, spring predictability barrier, optimal initial errors, optimal precursory disturbance**

**Citation:** Zhang J, Duan W S, Zhi X F. 2014. Using CMIP5 model outputs to investigate the initial errors that cause the "spring predictability barrier" for El Niño events. Science China: Earth Sciences, 57: 1−6, doi: 10.1007/s11430-014-4994-1

The El Niño-Southern Oscillation (ENSO) is a naturally occurring fluctuation that originates in the tropical Pacific region and has severe meteorological and social impacts worldwide (Torrence and Webster, 1999; Power et al., 1999). Our understanding of the dynamic and thermodynamic mechanisms of ENSO has been significantly advanced over recent decades. However, the predictability of ENSO events remains a subject of much debate, with the "spring predictability barrier" (SPB) being a particularly large and controversial problem in many coupled models (Jin et al., 2008). From a statistical perspective, the SPB refers to the fact that most ENSO prediction models often experience an apparent drop in anomaly-persistence corre-

*Corresponding author (email: duanws@lasg.iap.ac.cn)

lation skill during boreal spring (Webster and Yang, 1992; Latif et al., 1994; Webster, 1995; Lau and Yang, 1996; Torrence and Webster, 1998; Mc Phaden, 2003; Luo et al., 2008); while in terms of error growth, a "significant SPB" is a phenomenon through which ENSO forecasting possesses large prediction error and, in particular, a prominent error growth occurs during spring when the prediction is made prior to the spring (Mu et al., 2007a, 2007b; Duan et al., 2009; Yu et al., 2009).

The SPB remains a topic of ongoing research and debate, and its cause is yet to be fully understood (Jin et al., 2008). Some studies have argued that the SPB is an intrinsic characteristic of ENSO forecasting, while others have emphasized the role of initial errors in yielding the SPB, being possible to reduce it by improving the initial conditions. Moore and Kleeman (1996) investigated the season-dependent evolutions of initial errors related to the SPB and showed that the SPB may have a weak effect on ENSO predictability if the initial errors are slightly projected onto the fastest growing initial error. Chen et al. (2004) improved the initialization procedure of an ENSO forecast model and achieved much higher skill for ENSO forecasting, ultimately demonstrating that higher ENSO forecast skill depends more on the accuracy of the initial conditions than on unpredictable atmospheric noise, and further that more accurate initial conditions are much more beneficial for reducing the effect of the SPB on ENSO predictability.

Mu et al. (2007a, 2007b) showed that initial errors with a particular spatial structure are more likely to cause a notable SPB despite the existence of the climatological annual cycle in ENSO models. Duan et al. (2009) and Duan and Wei (2012) pointed out that such initial errors are often located in several key regions and may provide useful information regarding sensitive areas of adaptive observation for ENSO. That is, intensifying the observation networks in these sensitive areas identified by the initial errors, rather than other areas, and then significantly improving the accuracy of the initial fields, may lead to greatly improved ENSO forecast skill and the SPB's effect may be largely reduced (Yu et al., 2012). It is clear that the accuracy of the initial conditions is important for improving ENSO forecast skill, which also sheds light on the fact that initial errors, especially those with a particular spatial structure, are crucial in yielding the SPB for ENSO events. Nevertheless, all these results are derived from the intermediate coupled the Zebiak-Cane model (Zebiak and Cane, 1987), and should be verified by much more complete coupled general circulation models (GCMs). Accordingly, in this study we asked the following questions: (1) Does the phenomenon of the SPB for ENSO events exist in coupled GCMs? If so, what types of initial errors often cause the SPB of ENSO events? Are they similar to those obtained by the Zebiak-Cane model? (2) What useful information do the SPB-related initial errors provide for improving El Niño forecast skill?

We aim to address these questions by analyzing the outputs of several CMIP5 models. In particular, the response of atmospheric wind stress and subsurface temperature are used to explain the possible mechanism responsible for initial error growth. The remainder of the paper is structured as follows. In the next section we provide a brief introduction to the three CMIP5 models used, and the experimental strategy. In section 2, the season-dependent evolution of the initial errors is presented using the outputs of the three different coupled models, and then the characteristics of the initial errors often yielding a prominent SPB of El Niño forecasts are identified. Based on this, the implication for the role played by initial errors in the SPB is discussed in the context of adaptive observations. Finally, further discussion and a summary are presented in sections 4 and 5.

## 1 Strategy

The CMIP5 experiments provide useful model datasets for scientific studies used in the Intergovernmental Panel on Climate Change (IPCC) fifth Assessment Report (AR5; Taylor et al., 2012). This study attempts to use the model data to study the initial errors that often cause the SPB for ENSO predictions. Obviously, the expected model data can be extracted from the CMIP5 model outputs. In particular, the outputs of three models were chosen to derive the model data used in this paper. The three models have potential for yielding a significant SPB for El Niño predictions (see section 2.1). The corresponding models are listed in Table 1.

We use the monthly mean data of the pre-industrial (PI) control runs of the CMIP5 experiments, in which the sea surface temperature (SST), subsurface temperature (at depths of 5–155 m), and zonal and meridional wind components are derived from the outputs of the three models shown in Table 1. From the output of each model, we randomly chose three groups of 20-year SST time series, and in these SST time series we identified El Niño events of interest: a total number of nine events. These El Niño events tended to start in boreal spring and peak at the end of the year. For each 20-year time series, the SST in each El Niño year (from January to December) are respectively assumed

**Table 1** The three chosen CMIP5 coupled models

| Model | Full name | Institution |
|---|---|---|
| FGOALS-g2 | The Flexible Global Ocean-Atmosphere-Land System model, Grid-point Version 2 | LASG, IAP, Chinese Academy of Sciences; CESS, Tsinghua University |
| BCC-CSM1.1 | The Beijing Climate Center Climate System Model | Beijing Climate Center, China Meteorological Administration |
| NorESM1-M | The Norwegian Climate Center's Earth System Model | Norwegian Climate Centre |

to be the "observation"; then, any other 19-year SSTs are treated as 19 "predictions" for the "observed" El Niño year. This yields 171 predictions for 9 El Niño events for each model. The prediction errors are characterized by the differences between the "observed" El Niño and its "prediction". Specifically, the prediction errors $E(t)$ for El Niño events at a future time $t$ were calculated as follows:

$$E(t)=\left\|T^{P}(t)-T^{O}(t)\right\|=\frac{1}{N}\sqrt{\sum_{i,j}\left[T^{P}_{i,j}(t)-T^{O}_{i,j}(t)\right]^{2}}, \quad (1)$$

where the prediction errors are measured by the norm $\|\ \|$ shown in eq. (1), $T^{P}$ represents the "predicted" SST, $T^{O}$ denotes the "observed" SST, $(i, j)$ are the grid points in the Niño-3.4 region, and $N$ is the total grid number of the Niño-3.4 region. To explore the growth tendency of the prediction errors, we followed the Mu et al. (2007a) definition that the growth rate $k$ of prediction errors during a short period can be estimated by evaluating:

$$k=\frac{\partial E(t)}{\partial t}\approx\frac{E(t_2)-E(t_1)}{t_2-t_1}, \quad (2)$$

where $E(t_1)$ and $E(t_2)$ respectively represent the prediction errors at future times $t_1$ and $t_2$ ($t_2>t_1$, and $t_2$–$t_1$ is sufficiently small). A positive (negative) value of $k$ corresponds to an increase (decrease) of error, and the larger the absolute value of $k$, the faster the increase (decrease) of the error.

Since we adopted the PI control runs of the CMIP5 experiments with time-invariant forcing, the prediction errors of the "observed" El Niño events can be considered as being caused only by initial errors. Hence, we conduct here the first kind of predictability experiments to identify the role of initial errors in El Niño predictability.

## 2 Results

In this section we investigate the season-dependent evolution of prediction errors caused by initial errors for El Niño events and identify the initial errors that cause a significant SPB for El Niño events. The so-called significant SPB is recognized as a phenomenon in which ENSO forecasting possesses large prediction errors and, in particular, the prominent error growth occurs during spring when the prediction is made prior to the spring (Duan et al., 2009). In this paper, we refer to the initial errors that cause a significant SPB as "SPB-related optimal initial errors". By analyzing the evolution of these optimal initial errors, the mechanism of error growth associated with the SPB is identified. Furthermore, the usefulness of SPB-related optimal initial errors is analyzed in the context of adaptive observation.

### 2.1 The season-dependent evolution of prediction errors caused by initial errors

According to the strategy described in section 1, we used the outputs of the three models mentioned in section 1 and computed the prediction errors of the Niño-3.4 SST for "observed" El Niño events. By Eqs. (1) and (2), the growth rates of the prediction errors in each month were estimated. For the chosen three 20-year SST time series, we obtained similar results; so, for simplicity, we only present one of three 20-year time series for each model. Figure 1 shows the ensemble mean of the monthly growth rates of prediction errors of the Niño-3.4 SST for the El Niño events in one of three 20-year SST time series. From Figure 1 we can see that, for the FGOALS-g2, BCC-CSM1.1 and NorESM1-M models, the significant growth of SST prediction errors often occurs in the period June–August. That is, the prediction errors for El Niño events possess obvious season-dependent evolution, with the most significant growth starting in the period June–August. According to Mu et al. (2007a, 2007b) and Duan et al. (2009), an El Niño forecasting with significant error growth in spring and the beginning of summer causes the SPB phenomenon. We are able to demonstrate that the three models tend to yield the SPB phenomenon for El Niño forecasting. As mentioned in the introduction, the SPB is an essential characteristic of ENSO predictions. Therefore, the results shown in Figure 1 indicate that the

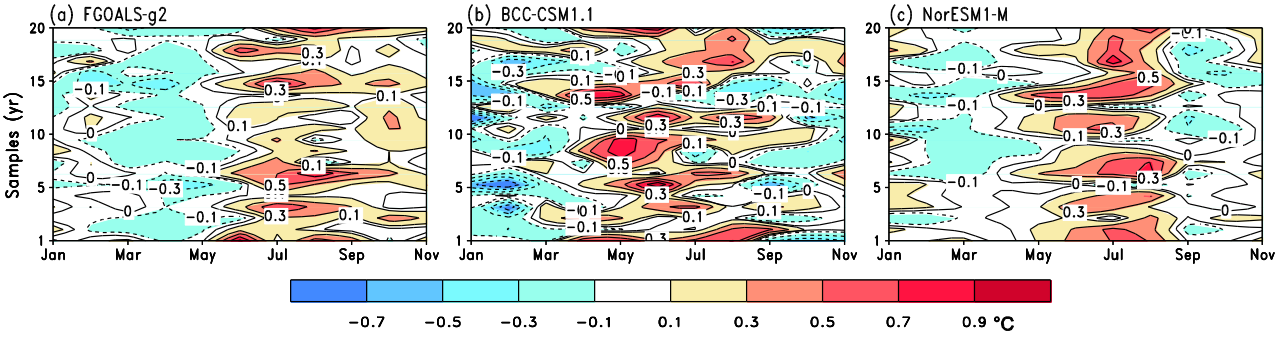


**Figure 1** Ensemble mean of the monthly growth rates of prediction errors of the Niño-3.4 SST for El Niño events in one 20-year SST time series. The vertical axes denote the samples of initial errors. The contour lines represent the monthly growth rates of the increase (or decrease) of prediction errors, where the positive values indicate the growth of the prediction. The growth rate of prediction errors in a given month was evaluated by subtracting the prediction error in this month from that in the next month.

three models (i.e. FGOALS-g2, BCC-CSM1.1 and NorESM1-M) are capable of capturing the characteristics of the SPB for ENSO predictions, and further that the initial errors may cause the SPB phenomenon.

By analyzing each of the above predictions for the El Niño events in these three models, we found that some of the predictions have obvious season-dependent evolution with significant growth occurring in June–August (especially in July and August) and yield an SPB phenomenon, while others present an insignificant season-dependent evolution of prediction errors and fail to cause the SPB (see Figure 2). As mentioned above, the prediction errors considered in this study are only caused by initial errors. We infer that some initial errors could cause the SPB while others fail to yield the SPB. That is, the SPB may be closely related to initial errors despite the annual cycle existing in the models. Nevertheless, from Figure 2, some initial errors are noticeably larger than 0.5°C and are not comparable to the realistic initial SST errors. Figure 3 shows the evolution of initial errors with amplitudes less than 0.5°C, it is still shown that some initial errors cause the SPB while others do not. To address the question of which features display the initial errors that often cause the SPB for El Niño events in the above coupled GCMs, we investigate the spatial structure of the initial errors that lead to a significant SPB for El Niño events.

### 2.2 The initial errors that cause a significant SPB for El Niño events

As demonstrated in section 2.1, the FGOALS-g2, BCC-CSM1.1 and NorESM1-M models indicate the SPB phenomenon for El Niño predictions. To explore the common characteristics of the initial errors that often cause the SPB for El Niño predictions, we examined those initial errors that present significant growth in boreal spring and also cause large prediction errors for El Niño events, i.e. we attempted to identify the SPB-related optimal initial errors

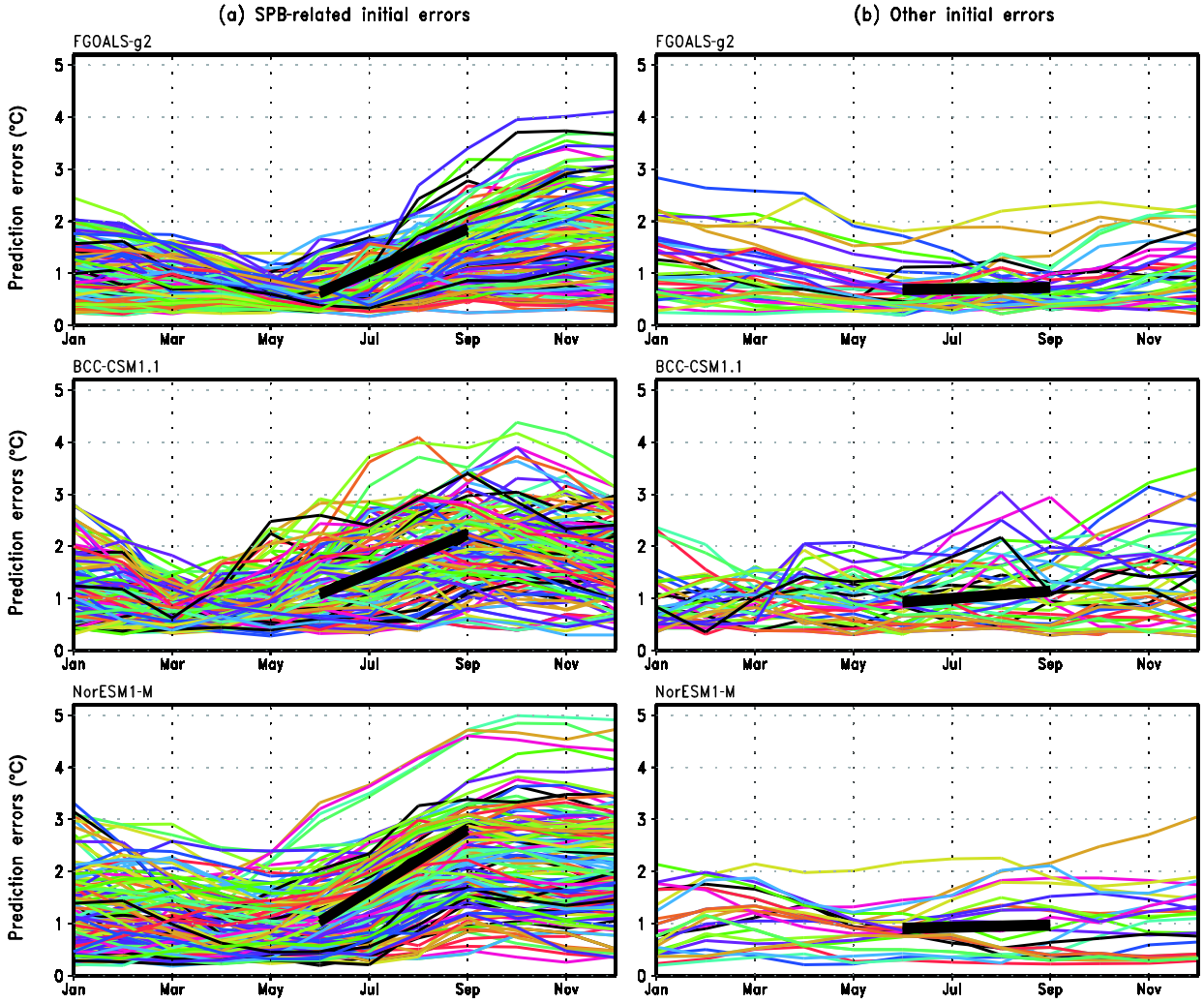


**Figure 2** The evolution of the prediction errors (curves) of the Niño-3.4 SST caused by the SPB-related initial errors (a) and other initial errors (b). The prediction errors caused by the SPB-related initial errors tend to present the significant growth (i.e. the large slope indicated by the short-thick line) in the period June–August, where the adopted model outputs are from the FGOALS-g2, BCC-CSM1.1 and NorESM1-M, respectively.

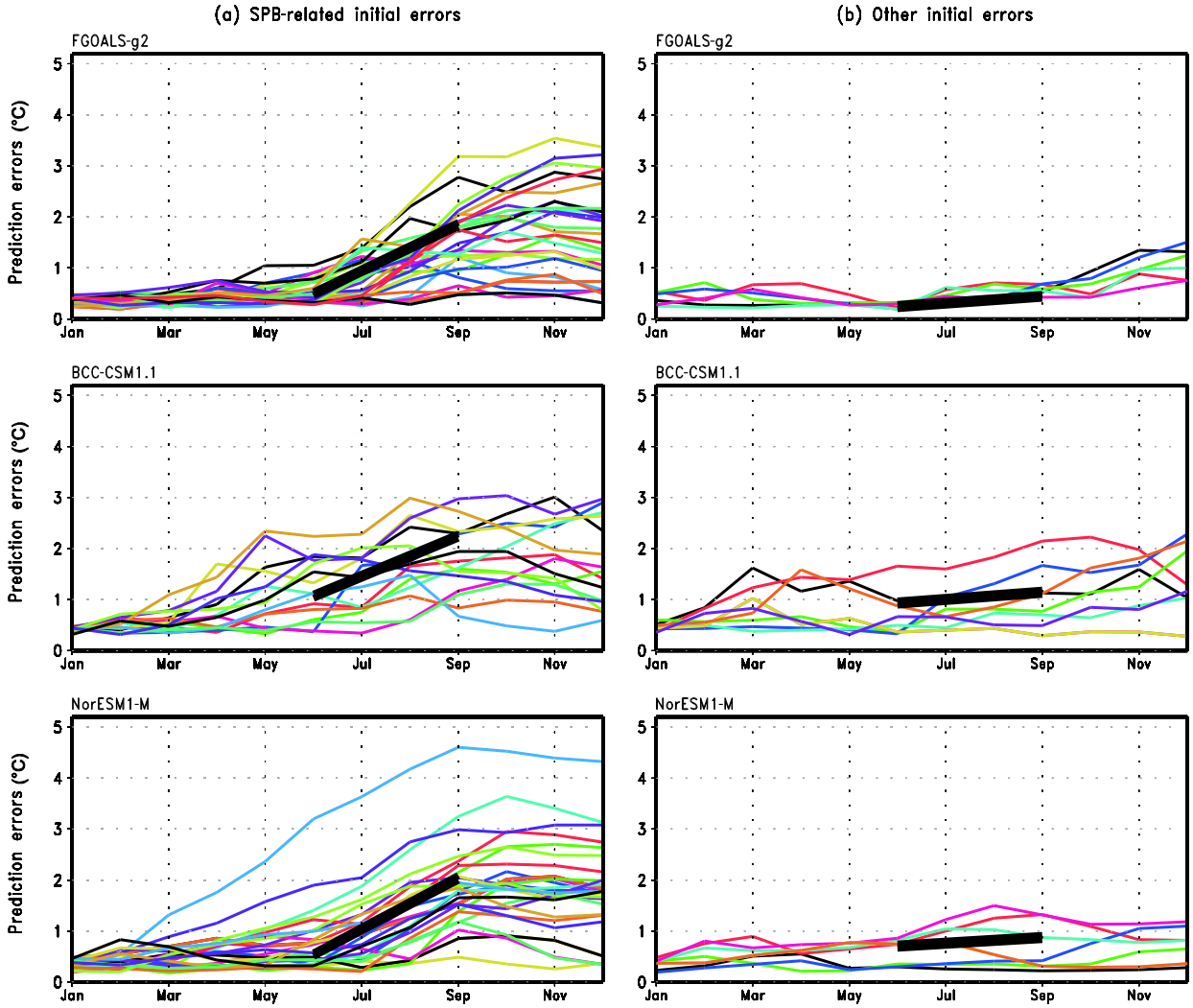


**Figure 3** As in Figure 2, except for the initial errors of Niño-3.4 SST with amplitudes less than 0.5°C.

(see section 2). Following this, we found that there does indeed exist a type of initial error which, when compared to other initial errors, is much more likely to cause a significant SPB and may act as the SPB-related optimal initial error. Figure 4 plots the composites of the SST and subsurface temperature components of the SPB-related optimal initial errors. It can be seen that this type of initial error, in any of the three models, often has an SST component with positive errors in the central-eastern equatorial Pacific, a subsurface temperature component with positive errors in the upper layers of the central-eastern equatorial Pacific, and negative errors in the lower layers of the western equatorial Pacific.

By tracing the evolution of the SPB-related optimal initial errors of the three models, we found that these initial errors often possess a La Niña-like evolving mode, yielding a cold bias for Niño-3.4 SST anomalies (SSTAs) of the El Niño events. In other words, the SPB-related optimal initial errors often cause the El Niño events to be under-predicted. For simplicity, in Figure 5 we only show the evolution of the SPB-related optimal initial errors of the FGOALS-g2 model. It can be seen that these SPB-related optimal initial errors first undergo a decaying period of El Niño and then a transition to a typical La Niña evolving mode. Physically, when these initial errors disturb the initial state of an El Niño event, a large but positive SST error initially occurs in the central-eastern equatorial Pacific, which increases the vertical temperature difference across the mixed layer base and causes $T'-T_e'$ to be greater than zero ($T'$ and $T_e'$ denote the errors superimposed on the SST and the entrained water temperature from beneath the mixed layer, respectively). In this situation, the perturbed vertical temperature advection induced by the mean upwelling would act against the positive SST error. Meanwhile, due to the effect of the SPB-related initial errors, a westerly perturbation occurs over the tropical central Pacific and in turn generates perturbed Rossby waves that propagate westward. These are reflected off the western ocean boundary and induce a perturbed upwelling Kelvin wave that travels eastward. In addition, a perturbed divergent wind also occurs around the dateline,

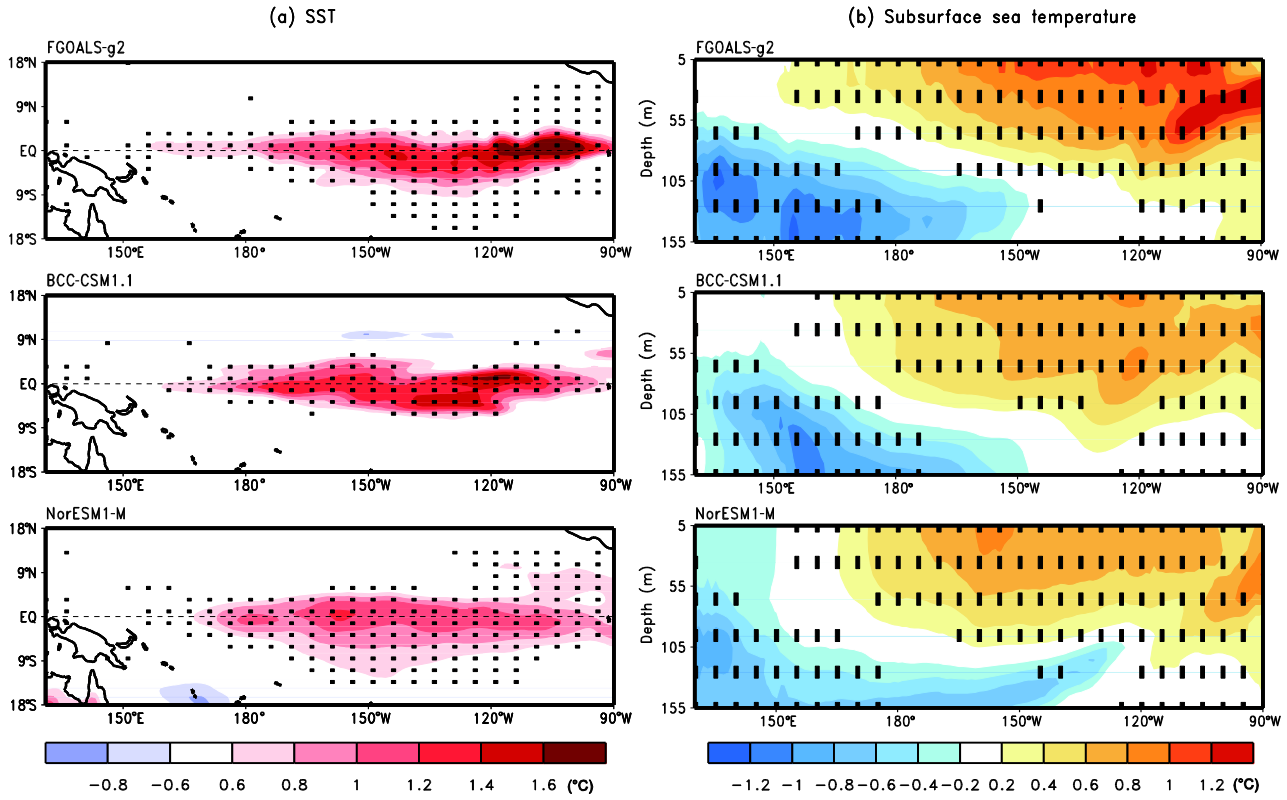


**Figure 4** Composites of SST (a) and subsurface temperature components (b) (meridional mean over 5°S–5°N) over the tropical Pacific Ocean of the SPB-related optimal initial errors. The dotted areas indicate composites of SST and subsurface temperature errors exceeding the 95% significance level. The model outputs are from FGOALS-g2, BCC-CSM1.1 and NorESM1-M, respectively.

which lifts the depth of the thermocline and generates the eastward Kelvin wave. These combined Kelvin waves are conducive to raising the thermocline and persistently lead an eastward transmission of water mass along it from January to December, see Figure 5(b). This allows the cold subsurface water mass in the western equatorial Pacific, characterized by the SPB-related optimal initial errors, to be transported into the surface layer of the eastern equatorial Pacific, and offsets the positive SST error over the tropical eastern Pacific. It is clear that the rising thermocline, together with the mean upwelling, would terminate the positive phase of the initial SST error and reverse it to a cooling stage. Once the negative phase of SST error occurs over the tropical eastern Pacific, the cooling is further amplified through the easterly perturbation and rising of the thermocline due to the Bjerknes positive feedback mechanism (Bjerknes, 1969), ultimately yielding a cold bias, and underestimating the El Niño events.

Accompanying the eastward Kelvin wave in the lower layers of the equatorial Pacific westward Rossby waves off the equator also occur, induced by the SPB-related optimal initial error. This leads to a transmission of positive subsurface temperature errors to the western Pacific Ocean. These positive errors of subsurface temperature may reflect off the western ocean boundary and induce a perturbed eastward Kelvin wave, which may possibly affect the ENSO events in the following years, instead of this year in question. That is, the off-equatorial western Rossby wave may have little effect on the La Niña-like evolving mode of the SPB-related initial errors. As a result, the cold bias in the lower layers of the western equatorial Pacific, spreading eastward along with perturbed Kelvin waves, plays an important role in the La Niña-like evolving mode of the SPB-related initial errors.

## 3 Implications

We have demonstrated that the SPB-related optimal initial errors tend to have patterns of the SST component with positive anomalies in the eastern equatorial Pacific, a subsurface temperature component with positive anomalies in the upper layer of the eastern equatorial Pacific, and negative anomalies in the lower layer of the equatorial western Pacific. Furthermore, such initial errors often present a La Niña-like evolving mode. We note that the SPB-related optimal initial errors are the initial perturbations superimposed on initial states of El Niño events. Furthermore, from the physics of their evolution, the effect of El Niño events on error growth may be less important than the climatological annual cycle (also see Mu et al., 2013). As such, we infer that, if such initial perturbations are superimposed on a normal year, they may also evolve into a La Niña event. In

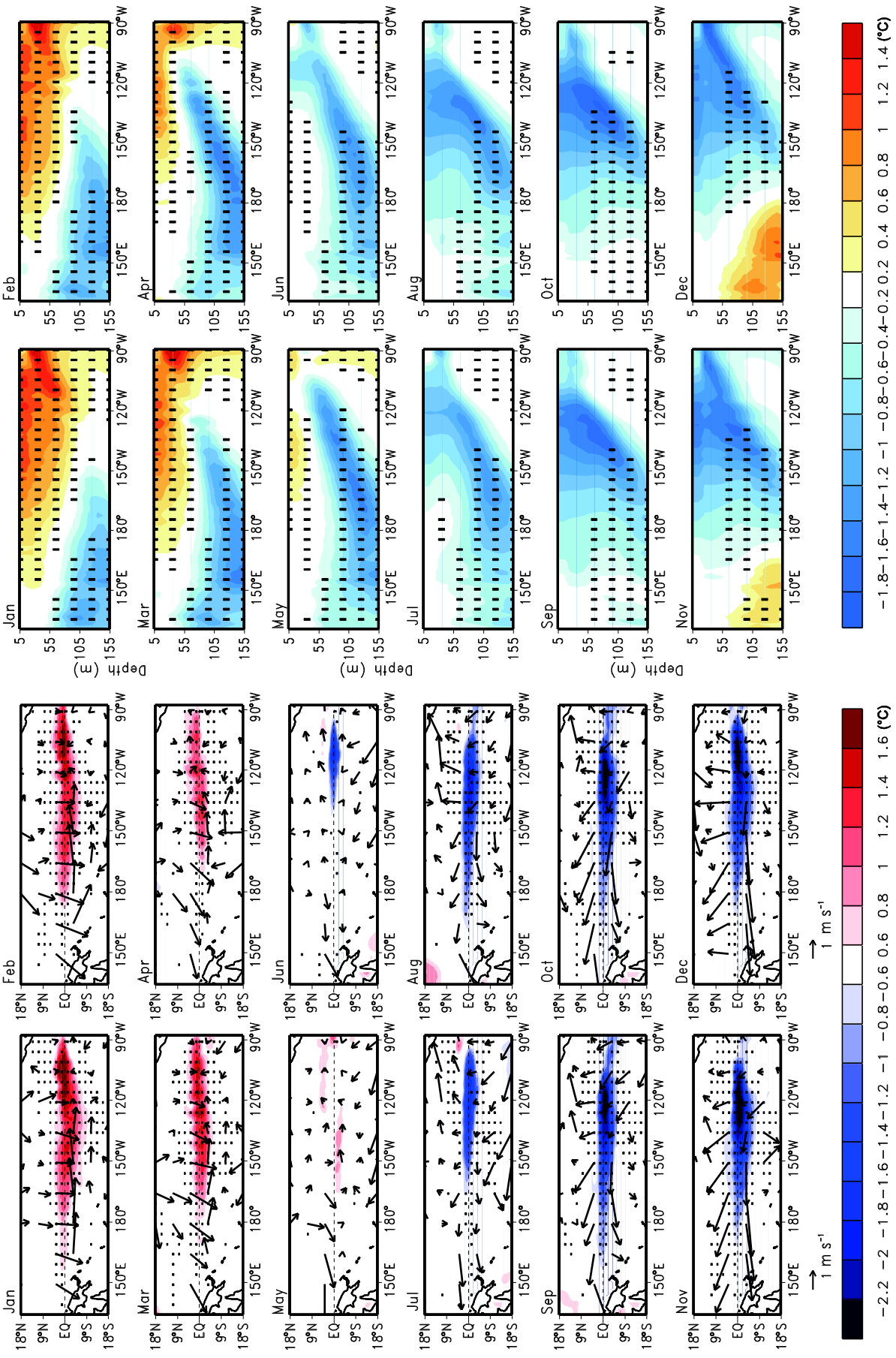


**Figure 5** Composites of the evolutions of the SPB-related optimal initial errors. (a) SST (units: °C) and horizontal wind (units: m s$^{-1}$) over the tropical Pacific Ocean; (b) Subsurface sea temperature (meridional mean over 5°S–5°N; units: °C). The dotted areas represent the composites of SST and subsurface temperature errors that exceed the 95% significance level. This result was obtained from the FGOALS-g2 model.

other words, the initial temperature anomaly that evolves into a La Niña event may have patterns similar to the SPB-related optimal initial errors. Conversely, could the initial temperature anomaly, with an almost opposite sign to the SPB-related optimal initial errors, develop into an El Niño event? If so, then the SPB-related optimal initial error and its opposite pattern may also play an important role in the optimal precursory disturbance of La Niña and El Niño events.

### 3.1 Similarities between the SPB-related initial errors and the optimal precursory disturbance of ENSO events

To confirm the above inference, we conducted another set of experiments. We adopted the strategy described in section 1, in particular by using the 20-year SST time series mentioned. In these SST time series, there exist not only El Niño and La Niña events, but also normal years. For each 20-year SST time series of each model, we assumed the SST in each normal year as a reference state to be predicted; then, the SST in El Niño and La Niña years were regarded as "predictions" for the reference state. So, the differences between initial values of the reference state (i.e. normal years) and those of the "predicted" El Niño and La Niña events could be regarded as the initial anomalies that were very likely to evolve into El Niño and La Niña events, respectively. For the initial anomalies associated with El Niño and La Niña, we performed a composite analysis. The results showed that the initial anomalies associated with El Niño possess the SST component with negative anomalies in the central-eastern equatorial Pacific, a subsurface temperature component with negative anomalies in the upper layers of the central-eastern equatorial Pacific, and positive anomalies in the lower layers of the western equatorial Pacific; while the initial anomalies associated with La Niña are usually of a temperature pattern almost opposite to the former. Figure 6 shows these two types of initial anomaly patterns for the three models. Correspondingly, Figure 7 plots the evolution of the initial anomalies shown in Figure 6, but only for FGOALS-g2. We see that the two types of initial anomalies do indeed evolve into typical El Niño and La Niña events, respectively. These two types of initial anomalies, since they correspond to almost all El Niño and La Niña events in the 20-year SST time series in the three models, can be considered as the optimal precursory disturbance for El Niño and La Niña, respectively. Furthermore, these two types of initial anomalies bear great resemblance with the SPB-related optimal initial errors. In particular, the SPB-related optimal initial errors are positively correlated to the optimal precursory disturbance for La Niña, with correlation coefficients of 0.857, 0.633 and 0.491 in the FGOALS-g2, BCC-CSM1.1 and NorESM1-M models, respectively. While the SPB-related optimal initial errors are negatively correlated with the precursory disturbance for El Niño with correlation coefficients of −0.686, −0.714 and −0.503. So, the SPB-related optimal initial errors are highly similar but negatively (positively) correlate to the optimal precursory disturbance for El Niño (La Niña) events.

### 3.2 Implications of the SPB-related optimal initial errors in the context of adaptive observation

Adaptive observation is an observing strategy that developed in the early 1990s. To better predict an event at a future time $t_1$ (the verification time) in a focused area (the verification area), additional observations are deployed at time $t_2$ (the targeted time; $t_2<t_1$) in some key areas (the sensitive areas), where additional observations are expected to have a considerable impact on the forecasts in the verification area (Snyder, 1996; Mu, 2013). A key problem in adaptive observation is the determination of the sensitive area where additional observations are expected to yield a better forecast than observations taken in other regions. Furthermore, given the high cost of observations over the ocean, a focus on a localized sensitive area may represent an economical and efficient strategy to improve the prediction skill of ENSO events.

In this paper we have illustrated that the SPB-related optimal initial errors tend to have an SST component with positive errors in the eastern equatorial Pacific, a subsurface temperature component with positive errors in the upper layers of the eastern equatorial Pacific, and negative errors in the lower layers of the western equatorial Pacific. From their evolutions, the growth of the negative prediction error of the Niño-3.4 SST for El Niño events is mainly induced by the contribution of the negative errors of subsurface temperature in the western equatorial Pacific; and then the negative errors of SST in the Niño-3.4 grow significantly due to Bjerknes positive feedback. As such, the prediction of El Niño may be highly sensitive to the initial errors in the areas associated with the subsurface layers of the western equatorial Pacific and the Niño-3.4 region. It is therefore reasonable to infer that the subsurface layers of the western equatorial Pacific and the Niño-3.4 region (see Figure 4), i.e. the areas where the SPB-related optimal initial errors are concentrated, may be the sensitive areas for the adaptive observation of ENSO events. Therefore, if additional observations are deployed in these two regions and the initial errors in the sensitive areas are reduced, the generation of large prediction errors may be avoided. In addition, we have also shown that the SPB-related optimal initial errors bear great resemblance to the optimal precursory disturbance for El Niño and La Niña events (see Figures 4 and 6). This implies such an improved observation network would be favorable for not only reducing the influence of the SPB on prediction uncertainties, but also for detecting the signals of the precursory disturbance triggering ENSO events.

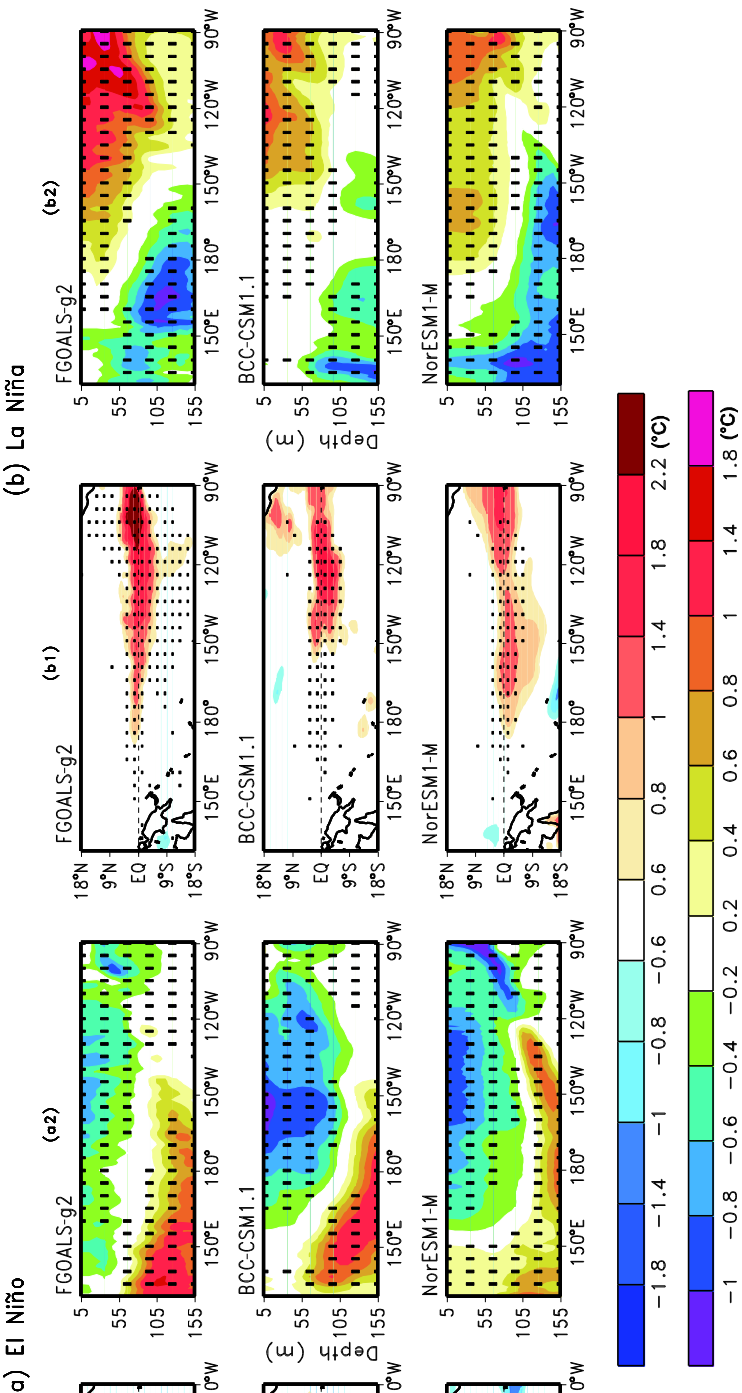


**Figure 6** Composites of the SSTA over the tropical Pacific Ocean and subsurface temperature anomaly components of the optimal precursory disturbance for El Niño (a) and La Niña (b) events. (a1), (b1) Composites of the SSTA (with the above color bar; units: °C); (a2), (b2) Subsurface temperature anomaly components (meridional mean over 5°S–5°N; with the below color bar; units: °C). The dotted areas represent the composites of SSTA and subsurface temperature anomalies that exceed the 95% significance level. The models are FGOALS-g2, BCC-CSM1.1 and NorESM1-M, respectively.

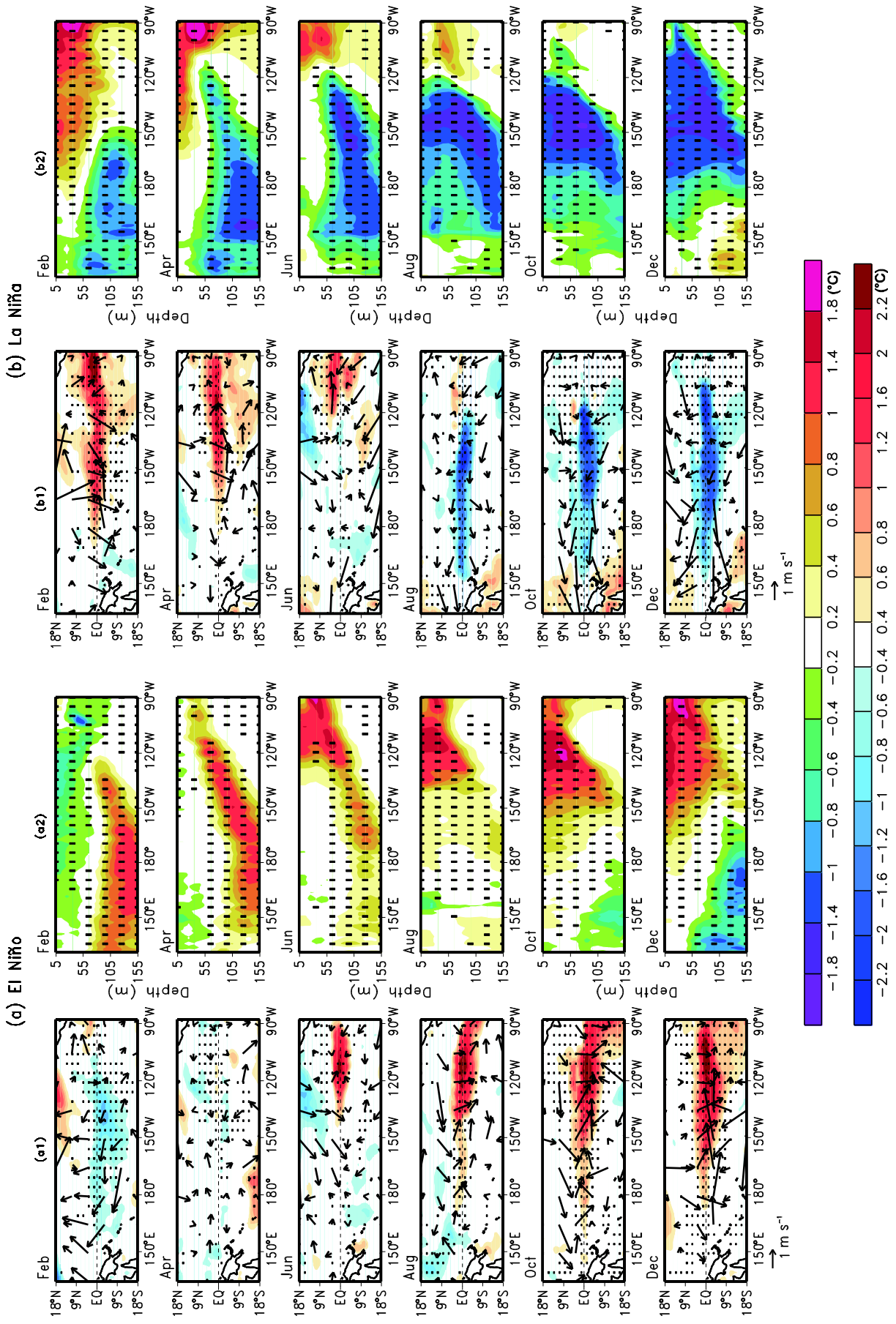


**Figure 7** Composites of the evolution of the optimal precursory disturbance for (a) El Niño and (b) La Niña events. (a1), (b1) the SSTA and surface wind anomaly over the tropical Pacific Ocean (with the above color bar; units: °C and m/s); (a2), (b2) Subsurface temperature anomaly components (meridional mean over 5°S–5°N; with the below color bar; units: °C). The dotted areas represent the composites of SSTA and subsurface temperature anomalies that exceed the 95% significance level. This result was obtained from the FGOALS-g2 model.

## 4 Discussion

Duan et al. (2012) explored the optimal precursory disturbance for El Niño events by using the intermediate-complex Zebiak-Cane model, which presents a SST pattern with positive anomalies in the eastern equatorial Pacific and negative anomalies in central-western equatorial Pacific and a deepening thermocline depth pattern along the equator. Mu et al. (2013) further showed, using the Zebiak-Cane model, that the optimally growing initial errors for El Niño events bear great resemblance with the optimal precursory disturbance for El Niño and La Niña events. Although the similarity between the precursory disturbance and optimally growing initial errors have also been shown in this study, the precursory disturbances for El Niño and La Niña events present different patterns from those obtained by the Zebiak-Cane model. To be specific, the precursors for El Niño exhibit an SST component with negative anomalies in the central-eastern equatorial Pacific, a subsurface temperature component with negative anomalies in the upper layers of the central-eastern equatorial Pacific, and positive anomalies in the lower layers of the western equatorial Pacific; while the precursors for La Niña are usually of a temperature pattern almost opposite to those for El Niño. As shown in the previous section, such precursory disturbances for El Niño (La Niña) events have a decaying period of negative (positive) anomalies in the eastern equatorial Pacific because of a negative feedback mechanism and then a transition to warm (cold) phase, finally growing into an El Niño (a La Niña) event due to the Bjerknes positive feedback. However, for the precursory disturbances obtained by the Zebiak-Cane model, the positive (negative) SST anomalies in the precursory patterns develop directly into an El Niño (a La Niña) event owing to the Bjerknes positive feedback. Therefore, the precursory disturbance obtained in this study may present a much earlier signal for the occurrence of El Niño and La Niña events than those obtained by the Zebiak-Cane model. That is to say, the precursory disturbances for El Niño and La Niña events obtained by the three CMIP5 models, compared to those obtained by the Zebiak-Cane model, are much optimal, and furthermore, very similar to the SPB-related optimal initial errors. Therefore, increasing observations in the sensitive areas identified by the SPB-related optimal initial errors not only reduces the influence of the initial errors on prediction uncertainties, but also better detects the signals provided by the ENSO's precursory disturbances determined by the three CMIP5 models. This is favorable to increasing the forecast skill of ENSO with a long lead time.

## 5 Summary

Using the monthly mean data of three model outputs in the CMIP5 experiments, this study investigated the spatial characteristics of the initial errors that often cause a significant SPB for El Niño forecasts. The results indicated that some initial errors exist that have obvious season-dependent evolution, with the significant growth occurring June through August, and tending to yield the SPB phenomenon. However, among these initial errors, the initial errors present obvious season-dependent evolutions and, furthermore, yield a large prediction error often presenting an SST pattern with positive errors in the central-eastern equatorial Pacific, a subsurface temperature pattern with positive errors in the upper layers of the eastern equatorial Pacific, and negative errors in the lower layers of the western equatorial Pacific. Such a kind of initial errors may therefore act as the SPB-related optimal initial errors; i.e., the initial errors that often cause a significant SPB for El Niño events. The SPB-related optimal initial errors may reflect the temperature pattern that arises in the transition period from El Niño to La Niña and exhibit a typical La Niña-like evolving mode, ultimately causing a cold bias for Niño-3.4 SSTAs of El Niño events.

We found that the cold bias caused by the SPB-related optimal initial errors originates from the lowers layer of the western equatorial Pacific and grows large in the eastern equatorial Pacific. Therefore, it is reasonable to hypothesize that the subsurface layers of the western equatorial Pacific with large errors, and in the Niño-3.4 region, may represent sensitive areas for the adaptive observation of El Niño events. That is, by reducing the initial errors in these two areas, the El Niño forecast skill may be greatly improved, compared to reducing the initial errors in other areas. This indicates that a priority should be given to deploying additional observations in these two areas for improving the ENSO forecasting skill. In addition, we showed that the SPB-related optimal initial errors are very similar to the optimal precursory disturbance for El Niño and La Niña events. We infer that improvement of the observation network by adaptive observations in the aforementioned sensitive areas could be of great help, not only in reducing the influence of the SPB on prediction uncertainties, but also in detecting the signals provided by the precursory disturbance triggering ENSO events, which may ultimately reduce the chance of false predictions of El Niño events and improve the skill of ENSO forecasting.

Duan et al. (2009) and Mu et al. (2013) used the Zebiak-Cane model to identify the sensitive areas of ENSO forecasting by tracing the growth of optimal initial errors of SSTA and thermocline depth anomaly. However, the thermocline depth anomaly couldn't be directly obtained by observation. Therefore, the above studies mainly focused on the sensitive areas for adaptive observation in the SST component. In this paper, we have instead used three CMIP5 models to identify the sensitive areas, not only for the SST component, but also for that of the subsurface temperature. Furthermore, these sensitive areas are also favora-

ble for detecting the signal of onset of ENSO events with a much longer lead time. Considering the fact that subsurface temperature transitions associated with ENSO lead to the SST (Wang and Fang, 1996), the lower layers of the western equatorial Pacific may provide much useful information for the sensitive areas of ENSO forecasting.

For the determination of the sensitive areas of ENSO forecasting, only the tropical Pacific temperature was used despite the SPB-related optimal initial errors being related to the global ocean and many other atmospheric and oceanic variables. Of course, considering the interactions among different basins of the Indian, Atlantic, and Pacific oceans, it is also worthwhile investigating the effect of these oceanic basins on the sensitive areas of ENSO forecasting. It is also necessary to examine the contributions of other atmospheric and oceanic variables to the predictability of ENSO events, and even the effect on the identification of sensitive areas. In the present study we simply used the model outputs of CMIP5 experiments to investigate the SPB-related optimal initial errors and indicate the sensitive areas for ENSO forecasting. Despite it being reasonable according to the physics, the existing model outputs cannot be used to confirm whether or not these sensitive areas are valid in adaptive observations. Therefore, further sensitivity experiments, e.g. by running numerical models, should be conducted to examine the validity of the identified sensitive areas in improving ENSO forecasting. Such work is underway in our group, and the preliminary results are encouraging.

*This work was jointly sponsored by the National Basic Research Program of China (Grant No. 2012CB955200), the National Public Benefit (Meteorology) Research Foundation of China (Grant No. GYHY201306018), and the National Natural Science Foundation of China (Grant Nos. 41230420, 41176013). Zhang Jing was supported by the Priority Academic Program Development of Jiangsu Higher Education Institutions (PAPD) and the Jiangsu Innovation Cultivation Project for Graduate Student (Grant No. CXZZ13_05).*

Bjerknes J. 1969. Atmospheric teleconnections from the tropical Pacific. Mon Wea Rev, 97: 163–172

Chen D, Cane M A, Kaplan A, et al. 2004. Predictability of El Niño over the past 148 years. Nature, 428: 733–736

Duan W S, Liu X, Zhu K Y, et al. 2009. Exploring initial errors that cause a significant spring predictability barrier for El Niño events. J Geophys Res, doi: 10.1029/2008JC004925

Duan W S, Wei C. 2012. The "spring predictability barrier" for ENSO predictions and its possible mechanism: results from a fully coupled model. Int J Clim, doi:10.1002/joc.3513

Duan W S, Yu Y Y, Xu H, et al. 2012. Behaviors of nonlinearities modulating El Niño events induced by optimal precursory disturbance. Clim Dyn, 40: 1399–1413

Jin E K, Kinter III J L, Wang B, et al. 2008. Current status of ENSO prediction skill in coupled ocean-atmosphere models. Clim Dyn, 31: 647–664

Lau K M, Yang S. 1996. The Asian monsoon and predictability of the tropical ocean-atmosphere system. Q J R Meteorol Soc, 122: 945–957

Latif M, Barnett T P, Cane M A, et al. 1994. A review of ENSO prediction studies. Clim Dyn, 9: 167–179

Luo J J, Masson S, Behera S, et al. 2008. Extended ENSO predictions using a fully coupled ocean-atmosphere model. J Clim, 21: 84–93

Moore A M, Kleeman R. 1996. The dynamics of error growth and predictability in a coupled model of ENSO. Q J R Meteorol Soc, 122: 1405–1446

Mc Phaden M J. 2003. Tropical Pacific Ocean heat content variations and ENSO persistence barriers. Geophys Res Lett, doi: 10.1029/2003GL016872

Mu M, Duan W S, Wang B. 2007a. Season-dependent dynamics of nonlinear optimal error growth and El Niño-Southern Oscillation predictability in a theoretical model. J Geophys Res, doi: 10.1029/2005JD006981

Mu M, Xu H, Duan W S. 2007b. A kind of initial errors related to "spring predictability barrier" for El Niño events in Zebiak-Cane model. Geophys Res Lett, doi: 10.1029/2006GL-27412

Mu M. 2013. Methods, current status, and prospect of targeted observation. Sci China Earth Sci, 56: 1997–2005

Mu M, Yu Y S, Xu H, et al. 2013. Similarities between optimal precursors for ENSO events and optimally growing initial errors in El Niño predictions. Theor Appl Climatol, doi: 10.1007/s00704-013-0909-x

Power S, Casey T, Folland C, et al. 1999. Inter-decadal modulation of the impact of ENSO on Australia. Clim Dyn, 15: 319–324

Snyder C. 1996. Summary of an informal workshop on adaptive observations and FASTEX. Bull Am Meteor Soc, 77: 953–961

Taylor K E, Stouffer R J, Meehl G A. 2012. Overview of CMIP5 and the experiment design. Bull Am Meteor Soc, 93: 485–498

Torrence C, Webster P J. 1998. The annual cycle of persistence in the El Niño Southern Oscillation. Q J R Meteorol Soc, 124: 1985–2004

Torrence C, Webster P J. 1999. Interdecadal changes in the ENSO- monsoon system. J Clim, 12: 2679–2690

Wang B, Fang Z. 1996. Chaotic oscillations of tropical climate: A dynamic system for ENSO. J Atmos Sci, 53: 2786–2802

Webster P J, Yang S. 1992. Monsoon and ENSO: Selectively interactive systems. Q J R Meteorol Soc, 118: 877–926

Webster P J. 1995. The annual cycle and the predictability of the tropical coupled ocean-atmosphere system. Meteor Atmos Phys, 56: 33–55

Yu Y S, Duan W S, Mu M. 2009. Dynamics of nonlinear error growth and season-dependent predictability of El Niño events in the Zebiak-Cane model. Q J R Meteorol Soc, 135: 2146–2160

Yu Y S, Mu M, Duan W S, et al. 2012. Contribution of the location and spatial pattern of initial error to uncertainties in El Niño predictions. J Geophys Res-Ocean, doi: 10.1029/2011JC007758

Zebiak S E, Cane A. 1987. A model El Niño-Southern Oscillation. Mon Weather Rev, 115: 2262–2278